Water Science & Technology

IWA PUBLISHING

Water Science & Technology Vol 85 No 4, 1321 doi: 10.2166/wst.2022.032

Novel scheme for synergistic purification of copper mine tailings and orthophosphate

Runjuan Zhou and Ming Zhang*

School of Architecture and Civil Engineering, Anhui Polytechnic University, Wuhu 241000, Anhui, P. R. China
*Corresponding author. E-mail: zhangming@ahpu.edu.cn

RZ, 0000-0003-0999-3638

ABSTRACT

Copper tailings (CTs) and orthophosphate are major environmental pollutants. CTs cause severe heavy metal pollution, and orthophosphate is one of the primary causes of water body eutrophication. This study aimed to alleviate heavy metal pollution by CTs and the eutrophication of water caused by orthophosphate. To this end, a 50 mg/L orthophosphate was used as a chemically active leaching solution and passed through a CT soil column. The tail water was then collected. Laboratory leaching tests showed that the thermally modified CTs effectively trapped orthophosphate, and the orthophosphate content in the leachate was 0.15 mg/L. After chemical washing, Cu^{2+}, Cd^{2+}, and Zn^{2+} were tested in the tail water, and the heavy metal ions in the tail water were removed using an advanced treatment technology. After treatment with 20.0 g/L water hyacinth biochar (WHBC), the removal rates (R%) of Cu^{2+}, Cd^{2+}, and Zn^{2+} were 99.48, 94.94, and 94.84%, respectively. These results demonstrated that this novel scheme for the synergistic purification of CTs and orthophosphate was feasible in the laboratory. This study provides new theoretical guidance and technical support for CT soil heavy metal remediation and water eutrophication treatment.

Key words: chemical washing, copper tailings (CTs), orthophosphate, synergistic purification, tail water

HIGHLIGHTS

- A novel soil column for repairing copper mine tailings and removing orthophosphate was constructed.
- Utilizing the synergistic purification effect between phosphorus-containing substances and heavy metals.
- The modified copper tailings have good adsorption performance for phosphate.
- Using the adsorbent to adsorb the heavy metals in the soil column leaching.
- Target biochar has good adsorption effect on target pollutants.

INTRODUCTION

Over the past 20 years, China has discharged or stacked nearly 60 billion tons of tailings, and more than 1.5 billion tons of tailings are discharged directly into the environment each year (Zeng *et al.* 2021). China is rich in mineral resources, with more than 8,000 state-owned mining enterprises and 230,000 collective mines producing a large amount of tailings and mining waste annually. The abandoned tailings may pollute farmland soil, surface water, groundwater, sediments, and surrounding plants and cause serious harm to the surrounding environment and the health of local residents (Wang *et al.* 2019). Currently, there are more than 12,000 copper tailing (CT) reservoirs in China; since 2009, the cumulative total of CTs in China has exceeded 10,000 metric tons (Mt) (Deng *et al.* 2017). China's copper industry has undergone rapid development in the twenty-first century, mainly reflected in the continuous expansion of industrial scale, the continuous strengthening of enterprises, and significant progress in some areas of technology. During ore dressing, the raw ore is usually processed through crushing, grinding, and chemical flotation to separate the minerals in the raw ore. However, the majority of CTs are produced after ore dressing, and most of these CTs are directly stacked in tailing reservoirs without advanced treatment or utilization. However, the tailings in reservoirs are easily eroded by wind and rain during the long stacking process. In addition, during the process of field stacking, the heavy metal elements in the tailings may leak into the surrounding environment, causing pollution and severe ecological damage. The stacking of CTs may lead to the heavy metal pollution of groundwater, which will increase water shortage pressure in China. Moreover, the direct stacking of tailings requires a large amount of land, which will indirectly reduce agricultural production and further aggravate global food shortages. An analysis of long-term monitoring data from tailing dams has shown

that the stability of these tailing dams is weak, and dam breaks can lead to serious disasters that harm human beings, the economy, and the environment (Dong *et al.* 2020; Lam *et al.* 2020; Yin *et al.* 2020). CTs are composed of fine-grained soil and the by-products of metallurgical processes. They release Cu, Cd, Cr, Pb, and other harmful heavy metals into the surrounding areas, causing harm to local land resources. These heavy metals spread through the food web, with potential toxic effects on animals, plants, and humans. Such toxicity is of particular concern (Munir *et al.* 2020). Therefore, while seeking better beneficiation technologies to reduce the heavy metal content in tailings, it is urgent to find a more appropriate treatment and disposal method for the large amount of tailings that has already been produced.

Currently, the resource utilization of CTs is mainly reflected in the use of construction materials for buildings and adsorbent material for sewage treatment (Esmaeili *et al.* 2020; Munir *et al.* 2020; Zeng *et al.* 2021). The utilization of CTs as building materials, such as bricks and supplementary cementitious materials, has achieved the resource utilization of CTs to a certain extent, but the technical aspects require further improvements. In addition, there may be a risk of heavy metal leaching when using CTs as building materials. Therefore, the management, disposal, and utilization of CTs pose critical challenges for the environmental governance of countries that have large copper production facilities.

Chemical washing is a feasible remediation technology for heavy metal–contaminated soil. Although chemical washing technology is an efficient, time-saving, and widely used method, its efficiency largely depends on the washing agents used. For different classes of washing agents, their remediation effects on heavy metal pollution vary. These effects mainly include passivation and sequestration. Some materials contain carboxyl and phosphonic acid groups that can form stable compounds with metal ions and thus stabilize them. However, after washing by some agents, the heavy metals in soils may transform from stable fractions to labile fractions, resulting in the increased fluidity and biological toxicity of heavy metals (Feng *et al.* 2020). The choice of washing agent is therefore very important. Phosphorus-containing substances have a good passivation effect on heavy metal ions in the soil, which has a great influence on changes in speciation (Gao *et al.* 2020; Feizi & Jalali 2021; Raklami *et al.* 2021; Teng *et al.* 2021; Wang *et al.* 2021). They can form relatively insoluble metal-phosphate deposits with heavy metals, thus immobilizing the heavy metals and reducing the bioavailability of heavy metal ions in the soil (Gao *et al.* 2020). In this study, a solution containing orthophosphate (such as KH_2PO_4) was used as the chemical washing agent. During the washing process, not only were the heavy metals in the tailings passivated but the nutrients P and K were also added to the barren tailings during the washing process.

The heavy metal ions in CTs, such as Cu^{2+}, have an effective affinity with phosphate (Song *et al.* 2016). The author has used unmodified CTs and thermally modified CTs to study the adsorption of phosphate, and the results have shown that thermally modified CTs have a better adsorption ability for phosphate (Zhou *et al.* 2018; Zhou *et al.* 2019). Jin *et al.* (2021a) modified CTs with lanthanum hydroxide ($La(OH)_3$) and used this to adsorb phosphate. They found that $La(OH)_3$-modified CTs displayed great improvement in adsorption performance for phosphate. Hence, the synergistic effect of CTs and phosphate washing solution can be leveraged to mitigate some of the environmental impacts associated with the disposal of CTs. However, after washing, some heavy metals are deposited in the tail water because of the adsorption, hydrolysis, and co-precipitation of metal ions (Tchatchouang *et al.* 2021), which may cause heavy metal pollution in the water. Therefore, some negative ecological effects may result from this treatment method. For the remediation of heavy metal pollution in the soil of tailing reservoirs, it is difficult to accomplish remediation goals using a single remediation technology. A combination of methods should be used to improve the effects of remediation. In this study, a soil column washing system was established to simulate the tailing environment. By utilizing the synergistic purification effect between phosphorus-containing substances and CTs, washing experiments were conducted using an orthophosphate-containing solution. The tail water was collected, and its water quality indexes were evaluated. Finally, three water hyacinth materials were used for the advanced treatment of the tail water so as to reduce the harm caused by heavy metal ions to the environment. This study not only provides an effective method for the recovery and utilization of solid waste from CTs, thereby reducing the harm of CTs to the environment, but also provides a new method for phosphorus removal that makes full use of the 'purification synergy' of the two pollutants. This method realizes the concept of 'treating waste with waste' and achieves the goal of cleaner production.

MATERIALS AND METHODS

Materials

The CTs and water hyacinth used in this study were collected from a concentrating mill in Tongling and the pond inside Anhui Polytechnic University in Wuhu, Anhui Province, China, respectively.

All chemicals used were purchased from Sinopharm Chemical Reagent Co., Ltd (Shanghai, China). The potassium dihydrogen phosphate (KH_2PO_4), 98% sulfuric acid (H_2SO_4), ammonium molybdate ($(NH_4)_6Mo_7O_{24}{\cdot}4H_2O$), potassium antimony oxide tartrate ($K(SbO)C_4H_4O_6{\cdot}1/2H_2O$), ascorbic acid, sodium hydroxide (NaOH), hydrochloric acid (HCl), and nitric acid (HNO_3) were all of analytical pure grade. All of the solutions required for the experiment were prepared with self-made ultrapure water.

Preparation of thermally modified CTs and water hyacinth materials

For the thermal modification of the CTs, they were placed in a muffle furnace and heated for 2 hours at 340 °C (Zhou *et al.* 2018). The dried water hyacinth stem and root tissues were crushed by a plant crusher. They were then screened by 100 mesh, placed into an air-blowing drying oven, and dried to a constant weight to obtain water hyacinth stem and root powder. The preparation method used for water hyacinth biochar (WHBC) is described in a previous report (Zhou *et al.* 2020). The water hyacinth between 0.5 and 1.0 cm was placed evenly into a high-temperature quartz boat and placed in a constant-temperature area of the temperature control tube furnace. According to the optimal conditions determined by the results of the previous report, the pyrolysis parameters were set as follows: the initial temperature was 25 °C, the pyrolysis temperature was 425 °C, the residence time was 3.09 h, and the heating rate was 19.65 °C/min.

CT chemical washing experiments with the orthophosphate solution

The eluvial column used in the experiment was made of a plexiglass material. The soil column was 8.0 cm in diameter and 30.0 cm in height. At the bottom of the soil column, two small holes with a diameter of 0.5 cm were provided to discharge the leachate. From the top to the bottom, the soil column consisted of one layer of 1 cm of geotextile to ensure that the leachate was evenly sprayed to the bottom of the tailings; 10 cm of thermally modified CTs, the main part of the soil column, which mainly reacted with orthophosphate; 1 cm of geotextile to effectively separate the upper CT sand from the lower fine sand; 6 cm of fine sand to better simulate the natural tailing reservoir environment; 1 cm of geotextile to separate the upper fine sand and the lower quartz sand; 3.0 cm of quartz sand; 1 cm of geotextile; 3.0 cm of gravel; and 1 cm of geotextile. The quartz sand and gravel served primarily as filters. The final filling height was 27 cm. The CT sand was placed on the top layer in order to be closer to the natural tailing reservoir environment and to ensure that the tailings and orthophosphates were in full contact, as if the fine sand layer was placed on the top, the orthophosphates could be intercepted. The soil column structure is shown in Figure 1(a), and the soil column washing experimental device is described in Figure 1(b).

The phosphorus-containing chemical washing agent consisted of 50 mg/L orthophosphate (KH_2PO_4) (Zhou *et al.* 2019). The orthophosphate solution was placed into a container and set on an iron platform. The flow rate was controlled to 0.80 cm/h, and the flow rate of leaching was controlled by the infusion flow rate regulator. The washing experiment was conducted in the soil column. The tail water was collected using a sampling flask and used as the experimental solution for subsequent advanced treatment experiments. The concentration of heavy metal ions in the tail water of the column outlet was determined by a Shimadzu ICPE-9000 inductively coupled plasma emission spectrometer, the concentration of phosphate in the tail water was determined by the molybdate blue spectrophotometric method, and the pH of the tail water was determined by a PHS-25 pH meter.

Advanced treatment of the tail water

Water hyacinth is rich in cellulose, hemicellulose, and various histone proteins, which can be used as the precursors of biochar. The authors of the present study have carried out numerous experimental studies on the adsorption of heavy metals by water hyacinth materials, and the results show that water hyacinth materials have a good adsorption and removal effect on heavy metals (Zhou *et al.* 2019; Zhou *et al.* 2020). Therefore, in this study, water hyacinth stem powder, root powder, and biochar (WHBC) were used to treat the tail water. The batch adsorption experiments were used to treat the tail water. The advanced treatment effects of the three materials (at dosages of 0.5, 1.0, 2.0, 5.0, 10.0, and 20.0 g/L) on the tail water were investigated. The material and 25 mL of tail water were added to a 100 mL centrifuge tube, and the solution was oscillated for 4 h at a temperature of 298 K and speed of 150 rpm/min. Each experiment was performed in triplicate, and the average results of the triplicate experiments were taken as the final experimental results. At the end of the experiments, a vacuum filter device was used to filter the samples, and the Shimadzu ICPE-9000 was used to determine the concentration

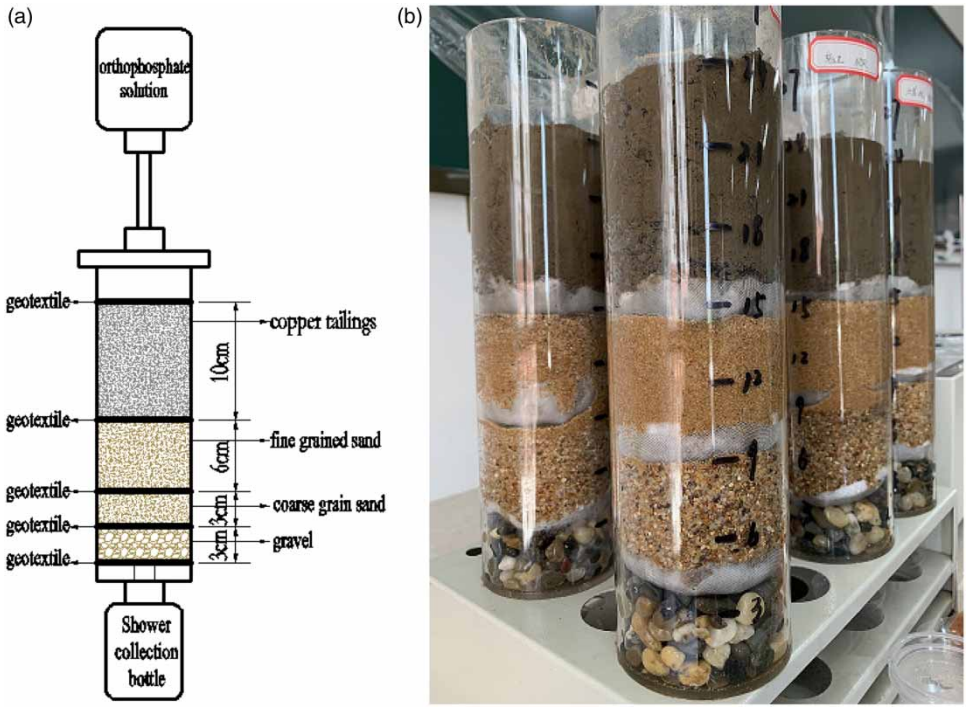

Figure 1 | (a) Diagram graph of the soil column washing, and (b) installation graphs of the soil column washing.

of heavy metal ions in the filtered samples. The removal rate ($R\%$) was determined using Equation (1):

$$R\% = \frac{C_0 - C_e}{C_0} \times 100\% \quad (1)$$

where C_0 and C_e represent the pollutant concentration in the influent and the effluent (mg/L), respectively.

Characterization of the materials

The characterization methods used for the water hyacinth materials are detailed in previous research (Zhou *et al.* 2018; Zhou *et al.* 2020). Scanning electron microscopy and energy dispersive spectroscopy (SEM-EDS) analysis was conducted using an S-4800 scanning microscope and an energy dispersive X-ray spectroscope (Hitachi, Japan) to examine the surface topography and the element types and contents of three water hyacinth materials. The materials were scanned and photographed 2,000 times and 5,000 times, respectively, under the condition of 5 kV high-acceleration voltage and vacuum extraction. The specific surface areas of water hyacinth materials were determined using a NOVA 2000e analyzer. Nitrogen adsorption-desorption was carried out in 77 K liquid nitrogen. The specific surface area and pore size distribution of the adsorbed material were calculated according to the peak areas of adsorption and desorption. The functional groups of materials were analyzed by a Shimadzu IRPrestige-21 transform infrared spectrometer (Shimadzu, Japan). Mix 1 mg sample powder with KBr at a mass of 1:200. After pressing, the samples were placed into the sample chamber and scanned at the wavelength range of 400–4,000 cm^{-1}. The crystallinity changes of the three materials were characterized by X-ray diffraction (XRD) with a Bruck-D8 series X-ray (powder) diffractometer (Bruck, Germany). A 0.2 g sample of powder was taken and placed into the sample chamber after tablet pressing and scanned in the range of 10°–80°.

RESULTS AND DISCUSSION

Composition analysis of the tail water in the soil column after chemical washing

After chemical washing, the pH, orthophosphate concentration, and heavy metal ion concentrations in the tail water were determined. The specific water quality indexes of the tail water are shown in Table 1, and the water quality index results are the average of triplicate experiments.

Table 1 | Water quality indexes of the tail water

Composition	pH	PO_4^{3-}	Cu^{2+}	Cd^{2+}	Zn^{2+}	Other heavy metal ions
Content	3.70	0.15 mg/L	130.25 mg/L	8.10 mg/L	21.50 mg/L	–

Note: '–' means not detected.

It can be concluded from Table 1 that the concentration of PO_4^{3-} in the tail water was 0.15 mg/L, which was lower than the first-level discharge standard of 0.5 mg/L in the 'Comprehensive Wastewater Discharge Standard' (GB8978-1996) and met the discharge standard. This standard is the national standard of China and is applicable to the management of pollutant discharge in existing water bodies nationwide. The results indicated that the CTs had a good interception effect on the phosphorus-containing wastewater and could reduce the risk of eutrophication. The pH of the tail water was 3.70, which belonged to the highly acidic wastewater category, and this pH was consistent with acid mine water exudate from actual tailing reservoirs. The concentrations of Cu^{2+}, Cd^{2+}, and Zn^{2+} in the tail water were 130.25, 8.10, and 21.50 mg/L, respectively, and other heavy metal ions were not detected. According to the 'Comprehensive Sewage Discharge Standard' (GB8978-1996), the prescribed concentrations for Cu^{2+}, Cd^{2+}, and Zn^{2+} are 1.0, 0.1, and 2.0 mg/L, respectively, and the concentrations of Cu^{2+}, Cd^{2+}, and Zn^{2+} greatly exceeded the prescribed standards. In general, the CT tail water was highly acidic. Hence, there is an urgent need for advanced treatment measures.

Following the use of chemical washing with orthophosphate, most of the phosphate was trapped in the tailings, and the phosphate concentration that leaked out was lower than the discharge standard. However, a portion of the heavy metal ions in the tailings leached into the tail water. This further confirms that during the process of tailing stacking and treatment, some heavy metal ions will leach out and cause heavy metal pollution to the surrounding environment. Therefore, it is necessary to conduct advanced treatment of these heavy metal ions to reduce harm to the environment.

Results of the advanced treatment of the tail water

The removal effects of the three materials on Cu^{2+} in the tail water are shown in Figure 2(a) and 2(b). It can be seen from Figure 2(a) that with an increase in the dosage of materials, the concentration of Cu^{2+} in the effluent showed a downward trend, and the removal rate of Cu^{2+} increased. The maximum removal rates of the stem powder, root powder, and WHBC were 63.89, 67.34, and 99.48%, respectively, and the effluent concentrations of Cu^{2+} were 47.03, 42.53, and 0.68 mg/L, respectively, when the adsorbent dosage was 20.0 g/L. It can be seen that the Cu^{2+} removal ability of WHBC was better

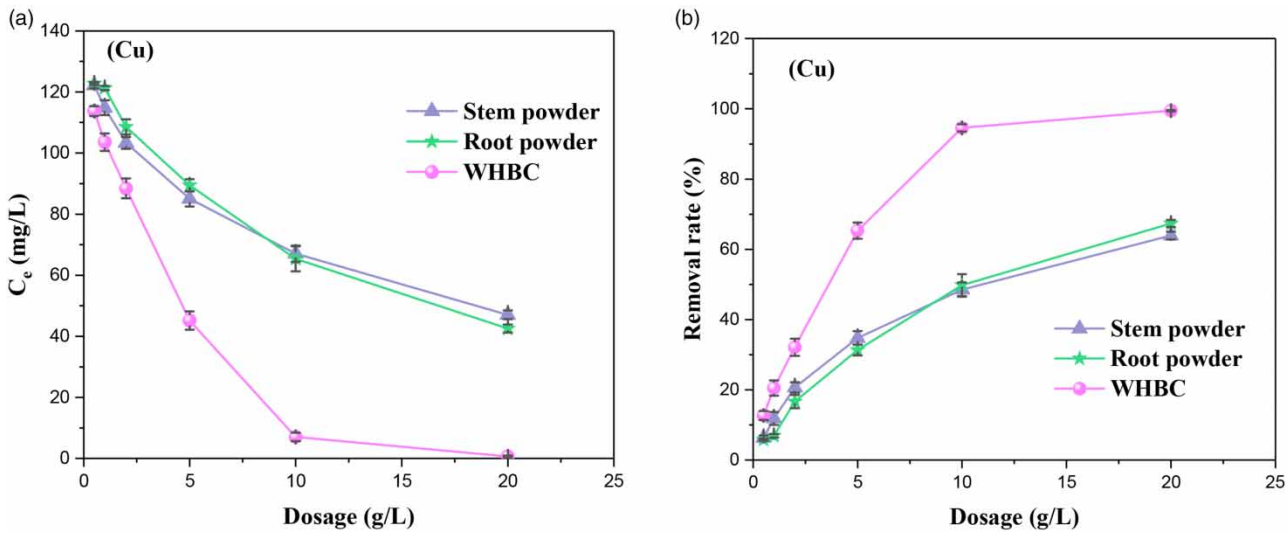

Figure 2 | Removal effect of Cu^{2+} by the stem powder, root powder, and water hyacinth biochar (WHBC): (a) effluent concentration and (b) removal rate.

than those of the stem and root powder. After advanced treatment using WHBC, the concentration of Cu^{2+} in the effluent was 0.68 mg/L, lower than the 1.0 mg/L in the secondary standard of the 'Comprehensive Wastewater Discharge Standard' (GB8978-1996).

Statistical Product and Service Solutions (SPSS) software was used to analyze the significance of the experimental results. A significance analysis of the Cu^{2+} removal efficiency of the three materials was conducted. The analysis results are described in Table 2. According to the analysis results, the Cu^{2+} removal efficiency of WHBC was significantly higher than those of the stem powder and root powder under different dosage conditions. The Cu^{2+} removal ability of stem powder was slightly better than that of root powder at medium and low dosages, while the Cu^{2+} removal ability of stem powder was lower than that of root powder at a high dosage. Overall, the significance analysis also showed that WHBC had a better removal effect than the stem powder and the root powder.

The Cd^{2+} removal effects of the three materials are displayed in Figure 3(a) and 3(b). As shown in Figure 3, compared with WHBC, the stem powder and root powder had poor removal effects on Cd^{2+} in the tail water. When the amount of adsorbent was 20.0 g/L, the removal rates of Cd^{2+} were only 48.02 and 54.39% for stem and root powder, respectively, and the effluent concentrations were 4.21 and 3.69 mg/L, respectively. The Cd^{2+} removal efficiency of WHBC increased with an increase in the dosage. When it increased to 20.0 g/L, the R% of Cd^{2+} in the tail water by WHBC was 94.94%, and the concentration of Cd^{2+} in the effluent was 0.41 mg/L, which was higher than the maximum allowable discharge standard of 0.1 mg/L (GB8978-1996). However, this would reduce the pressure for subsequent processing and the environmental risk.

The significance analysis results of the adsorption effect of Cd^{2+} are shown in Table 3. In general, the removal rate of WHBC on Cd^{2+} was significantly better than that of the stem and root powder at all adsorbent dosages. When the dosage

Table 2 | Significance analysis results of the removal efficiencies of Cu^{2+} by the three materials

	Adsorbent dosage (g/L)					
Materials	**0.5**	**1.0**	**2.0**	**5.0**	**10.0**	**20.0**
Stem powder	6.244 ± 0.692b	11.823 ± 1.862b	20.640 ± 1.484b	34.728 ± 1.931b	48.522 ± 2.043b	63.890 ± 1.089c
Root powder	5.758 ± 0.366b	6.859 ± 0.516c	16.622 ± 1.890c	31.312 ± 1.531c	49.776 ± 3.130b	67.345 ± 1.020b
WHBC	12.578 ± 1.250a	21.258 ± 1.054a	32.915 ± 1.482a	66.031 ± 1.464a	94.724 ± 0.987a	99.467 ± 0.192a

Note: Data in the table are mean ± standard error; different letters (lowercase letters represent a 5% significance level in the same column indicate that the adsorption effect of the three water hyacinth materials on heavy metal ions is significantly different under the condition of the same amount of adsorbent (p<0.05), and the same for Tables 3 and 4. Water hyacinth biochar: WHBC.

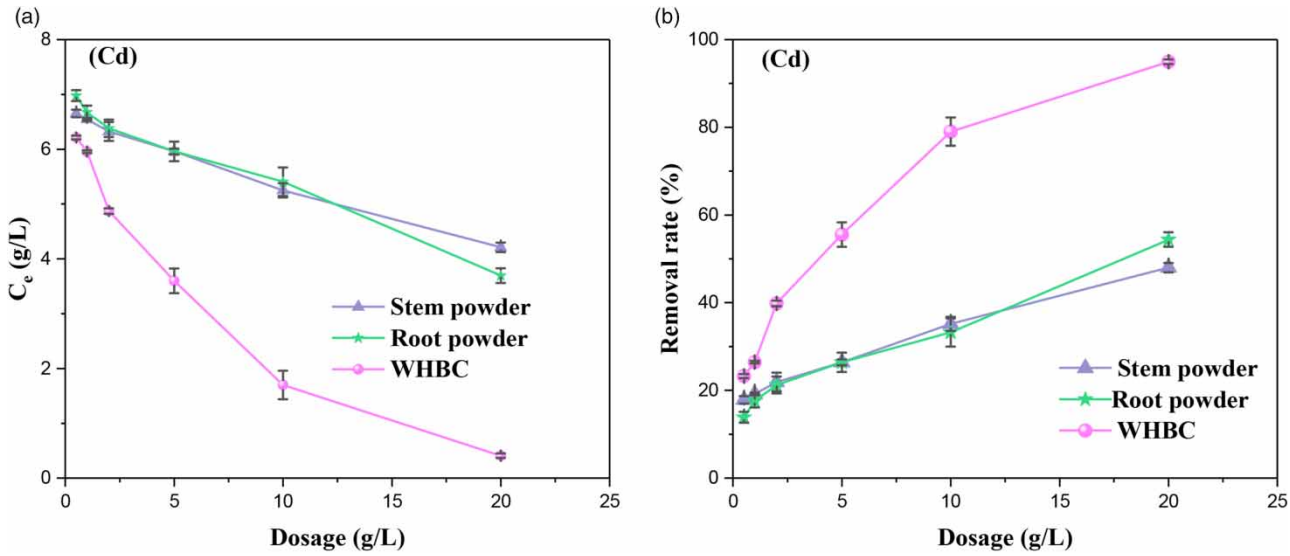

Figure 3 | Removal effect of Cd^{2+} by the stem powder, root powder, and WHBC: (a) effluent concentration, (b) removal rate.

Table 3 | Significance analysis results of the removal efficiency of Cd^{2+} by the three materials

	Adsorbent dosage (g/L)					
Materials	**0.5**	**1.0**	**2.0**	**5.0**	**10.0**	**20.0**
Stem powder	17.860 ± 0.840b	19.218 ± 0.311b	21.934 ± 2.125b	26.420 ± 0.653b	35.185 ± 1.614b	48.025 ± 1.076c
Root powder	13.868 ± 1.237c	17.613 ± 1.473b	21.235 ± 1.940b	26.420 ± 2.195b	33.251 ± 3.230b	54.399 ± 1.662b
WHBC	23.292 ± 0.434a	26.461 ± 0.285a	39.835 ± 0.634a	55.556 ± 2.791a	79.012 ± 3.217a	94.942 ± 0.527a

was 0.5–2.0 g/L, the Cd^{2+} removal effect of root powder was lower than that of the stem powder. When the dosage was higher than 5.0 g/L, the use of the root and stem powder for the Cd^{2+} removal effect did not show obvious differences, and the Cd^{2+} removal effect of the root powder was slightly higher than that of the stem powder. In addition, under the condition of a dosage of 20.0 g/L, the root powder was superior to the stem powder for the removal efficiency of Cd^{2+}. The significance analysis showed that WHBC had a better removal effect than the stem powder and the root powder.

After the tail water was treated with the three materials, the effluent concentrations and removal efficiency of Zn^{2+} were measured (Figure 4(a) and 4(b)). With increasing dosage, the Zn^{2+} removal rates of the three materials were also gradually enhanced. When the dosage reached 20.0 g/L, the Zn^{2+} removal rates of the stem powder, root powder, and WHBC were 43.41, 48.84, and 94.84%, respectively, and the effluent concentrations were 12.17, 11.0, and 1.11 mg/L, respectively. After treatment with the stem and root powder, the effluent concentrations were all higher than the 5.0 mg/L of the third-level discharge standard of the 'Comprehensive Wastewater Discharge Standard' (GB8978-1996), while the effluent concentration after WHBC treatment was lower than the 2.0 mg/L of the first-level discharge standard of the 'Comprehensive Wastewater Discharge Standard' (GB8978-1996).

The significance analysis results of the removal of Zn^{2+} from the tail water by the three materials are shown in Table 4. Under all the dosage conditions, the Zn^{2+} removal effect of WHBC was significantly stronger than those of the stem powder and root powder, and the removal effect of the root powder on Zn^{2+} was obviously better than that of the stem powder. According to the significance analysis, the Zn^{2+} removal effects of the three materials on the tail water were WHBC>root powder>stem powder.

Characterization of the water hyacinth materials

To further demonstrate that biochar had a better treatment effect on tail water than stem powder or root powder, the properties of the three materials before the treatment of tail water were characterized.

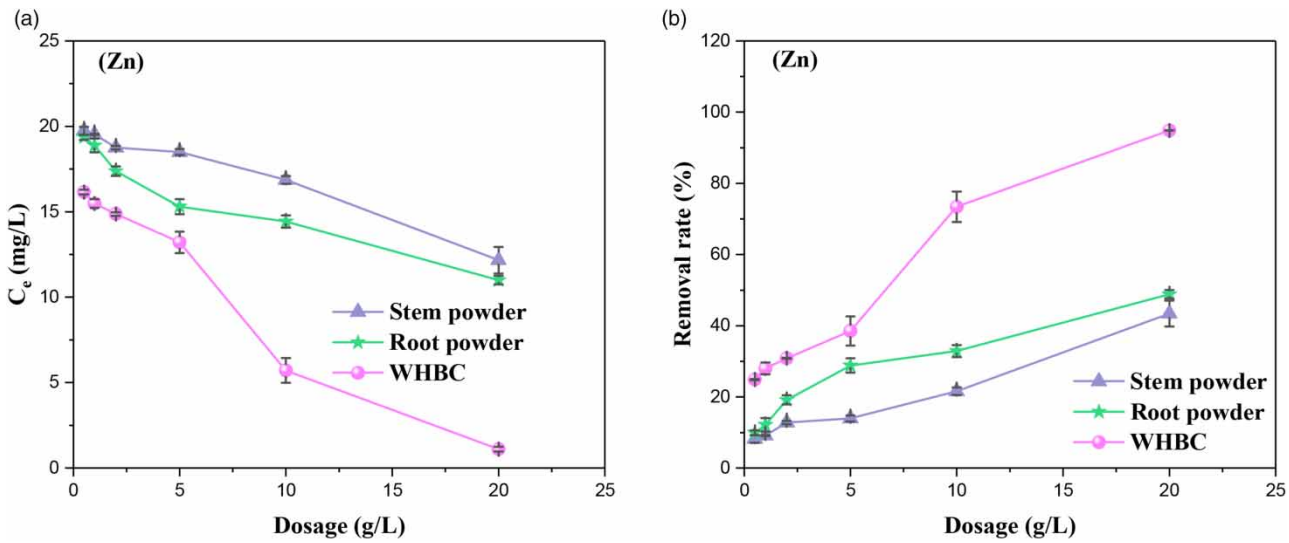

Figure 4 | Zn^{2+} removal effect of the stem powder, root powder, and water hyacinth biochar (WHBC): (a) effluent concentration and (b) removal rate.

Table 4 | Significance analysis results of the removal efficiency of Zn^{2+} by the three materials

	Adsorbent dosage (g/L)					
Materials	**0.5**	**1.0**	**2.0**	**5.0**	**10.0**	**20.0**
Stem powder	8.217 ± 1.099c	9.147 ± 0.134c	12.791 ± 0.465c	13.953 ± 0.806c	21.550 ± 1.049c	43.411 ± 3.613c
Root powder	9.922 ± 0.710b	12.171 ± 1.880b	19.147 ± 1.281b	28.837 ± 2.027b	32.868 ± 1.682b	48.837 ± 1.163b
WHBC	24.884 ± 0.615a	27.984 ± 1.171a	30.853 ± 0.484a	38.527 ± 2.926a	73.411 ± 3.365a	94.837 ± 0.646a

pH and the zeta potential of the three water hyacinth materials

The pH of the three water hyacinth materials was determined by pH meter (PHS-25, LEICI, Shanghai, China). The materials were mixed with ultrapure water at a mass ratio of 1:10 after oscillating at a speed of 150 r/min at 25 °C for 24 h. They were then filtered and the pH of the filtrate was measured.

The pH values of the stem powder, root powder, and WHBC were 6.53, 7.65, and 9.73, respectively. The pH values of the root powder and WHBC were in the alkaline range, which to some extent provided a good alkaline environment for the precipitation of Cu^{2+}, Cd^{2+}, and other heavy metal ions, improving the heavy metal removal performance. Biomass materials, such as biochar prepared with aquatic plants as raw materials, are generally alkaline and are used to treat acidic wastewater without washing to neutralize it, thus reducing the use of neutralizing agents and saving the cost of wastewater treatment. Therefore, whether to treat the biomass material can be decided according to the pH of the wastewater. In the treatment of acidic mine wastewater (tail water) or acidic industrial wastewater containing heavy metals, if the biomass material prepared is alkaline, no additional technical means are required to alter the pH so as to neutralize the acidic wastewater and reduce the treatment cost.

Precipitation is one of the mechanisms for removing heavy metal ions by materials. According to the solubility product constant (K_{sp}) of the metal hydroxide, the pH of the metal hydroxide precipitation at different concentrations can be calculated. The calculation equation is as follows:

$$\mathrm{pH} = \frac{1}{n} lgK_{sp} - lgK_{w} - \frac{1}{n} lg\alpha_{M^{n+}} \tag{2}$$

where K_{sp} and K_{w} are the solubility product constant of the metal hydroxide and the ion product constant of water, respectively, and $\alpha_{M^{n+}}$ is the concentration of metal ions (mol/L), where M represents the metal ion and n represents the valence of the metal ion.

At a room temperature of 25 °C, the *Ksp* values of $Cu(OH)_2$, $Cd(OH)_2$, and $Zn(OH)_2$ were 5.0×10^{-20}, 2.2×10^{-14}, and 7.1×10^{-18}, respectively, and the K_w was 1.0×10^{-14}. The concentrations of Cu^{2+}, Cd^{2+}, and Zn^{2+} in the tail water were 130.25, 8.10, and 21.50 mg/L, respectively. According to Equation (2), the pH values of the $Cu(OH)_2$, $Cd(OH)_2$, and $Zn(OH)_2$ precipitate were calculated to be approximately 5.70, 9.24, and 7.17, respectively. For Cu^{2+}, the pH values of precipitation were all lower than those of the three water hyacinth materials; in particular, they were much lower than that of WHBC. Cu precipitates were found in all three materials, but more precipitates were found in WHBC. For Cd^{2+}, the pH value of the precipitate was slightly lower than that of WHBC, so only a small amount of Cd was precipitated in WHBC. The pH value of Zn^{2+} precipitation was lower than those of the root powder and WHBC, but higher than that of the stem powder, so no Zn^{2+} was precipitated from stem powder. In general, the pH values of the three heavy metal ions precipitated in the tail water were all lower than that of WHBC.

The pH_{pzc} of water hyacinth materials was determined by a Zetasizer Nano ZEN3690 (Malvern Panalytical, UK) and measured using 0.01 M NaCl aqueous solutions in the pH range from 2.0–11.0. These pH values were fixed with 0.1 mol/L HCl and NaOH aqueous solution. The suspension was injected into the sample tank with a syringe, the zeta potential was measured in the sample tank, and the curve of the zeta potential changing with pH was drawn. When the zeta potential was 0, the corresponding pH was the point of zero charge of the material (pH_{pzc}) (Melliti *et al.* 2021).

The zeta potentials of the water hyacinth materials are displayed in Figure 5. According to the zeta potential analysis, the pH_{pzc} values of the stem powder and the root powder were not found in the measured pH range, and the pH_{pzc} of WHBC was

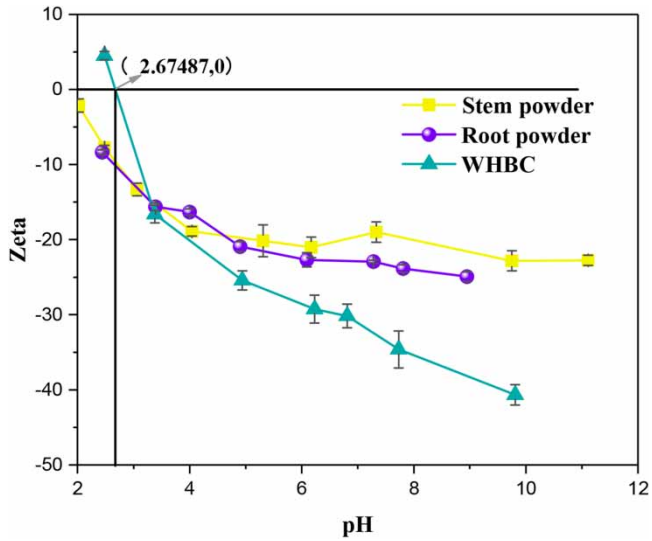

Figure 5 | Zeta potential of the water hyacinth materials.

2.67. The variations of zeta potential of the three water hyacinth materials may have been caused by the cracking of cellulose, hemicellulose, and lignin in water hyacinth after pyrolysis, which leads to the change of pH and surface functional groups, and further changes in the zeta potential. When the pH was higher than 2.67, the surface of WHBC was negatively charged, which favored the adsorption of positively charged heavy metals onto the WHBC surface (Melliti *et al.* 2021).

SEM-EDS spectra of the three water hyacinth materials

The SEM images of the stem powder, root powder, and WHBC at the same magnification are shown in Figure 6. The images showed that there were many fine particles on the surface of the stem powder that were smooth, and no obvious pore structure was found. However, the surfaces of the root powder and WHBC were rougher than the stem powder. In general, materials with rough surfaces are more likely to adhere to pollutants, so the rough surface is more conducive to the attachment of heavy metal ions. Therefore, structures of the root powder and WHBC are more conducive to the adhesion of heavy metal ions. There were more lamellar stacks and thinner lamellae in the WHBC, which may have been due to the rupture of the aliphatic hydrocarbon group and the lipid C=O functional group under the protection of the aromatic nucleus. These lamellar structures were different in size and formed more holes (shown in the red circle in Figure 6). In the case of an adsorption reaction, these structures could provide more sites for heavy metal ions and improve the removal effect. After high-temperature pyrolysis, cellulose, hemicellulose, and lignin in WHBC were cracked, which made the pore structure of WHBC more developed. Some spherical crystals appeared and the surface became rougher, which was more conducive to the attachment of heavy metal ions. In addition, after high-temperature pyrolysis, the dendritic cellulose in water hyacinth

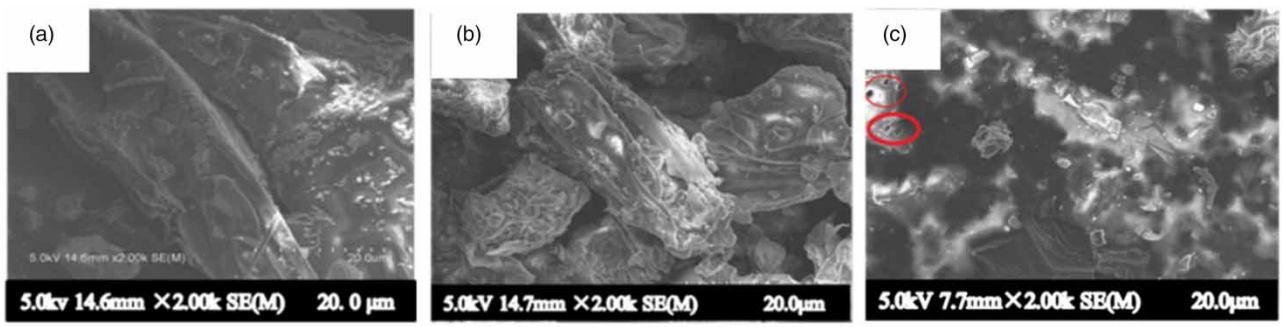

Figure 6 | Electron microscope scanning images of the (a) stem powder, (b) root powder, and (c) water hyacinth biochar (WHBC).

Table 5 | Elemental composition and percentage of the three materials

Element (Wt%)	Stem powder	Root powder	WHBC
C	65.83	55.56	53.72
O	24.47	24.74	16.82
Cl	4.58	7.16	2.47
K	5.11	6.73	9.24
Mg	–	–	3.49
Ca	–	–	6.23
P	–	–	8.03
Si	–	3.61	–
Al	–	2.20	–
Totals	100	100	100

will shrink, making the material surface become rough. Microspherical hemicellulose melts and foams, and its pore structure expands continuously. With the increase of temperature, organic components in lignin gradually exfoliate, pore structure becomes more developed, and spherical crystals appear. These changes improve the biochar's ability to capture and adsorb heavy metals.

On the basis of the SEM analysis, the stem powder, root powder, and WHBC were analyzed using X-ray energy spectra (EDS), and the element types and contents of the materials were determined. The EDS of the three materials are shown in Table 5. The results showed that the three materials all contained the elements C, O, Cl, and K. In addition to the above elements, the root powder contained small amounts of Si (3.61%) and Al (2.20%). The WHBC contained Mg (3.49%), Ca (6.23%), and P (8.03%), while the stem powder did not contain Si, Al, Mg, Ca, or P elements.

Brunauer–Emmett–Teller (BET) (specific surface area) and pore size distribution of the three water hyacinth materials

According to the data in Table 6, the surface areas of the stem powder, root powder, and WHBC were 0.216, 325.262, and 4.299 m^2/g, respectively. The surface area of the WHBC was smaller than that of the root powder, probably because the stem accounted for a larger proportion in the raw material.

The nitrogen adsorption-desorption curves of the three materials are shown in Figure 7(a) and 7(b). As shown in Figure 7(a), the curves of the stem powder and the WHBC conformed to a type-IV with H3-type hysteresis loop. Type-IV isotherms are derived from mesoporous adsorbent materials with multilayer adsorption and capillary condensation phenomena (Kaur *et al.* 2020). According to the analysis in Figure 7(b), the nitrogen adsorption-desorption curve of the root powder basically conformed to the type-IV with H3-type hysteresis regression curve, which also belonged to the mesoporous adsorbent materials, but the degrees of adsorption and desorption were similar.

Fourier-transform infrared spectroscopy (FTIR) spectra of the three water hyacinth materials

The qualitative differences in the surface functional groups of the three materials were analyzed using FTIR. The spectra are shown in Figure 8(a). The peak shapes of the three materials had many similarities, and all had stretching vibrations near 3,419 cm^{-1} (-OH), 2,369 cm^{-1} (C≡C), 1,645 cm^{-1} (-COO-), 1,089 cm^{-1} (-CO), and 832 cm^{-1} (-CH) (Rahman *et al.* 2019).

Table 6 | Surface areas, pore volumes, and pore diameters of the three materials

Samples	Surface area (m^2/g)	Pore volume (cm^3/g)	Pore diameter (nm)
Stem powder	0.216	0.002	8.494
Root powder	325.262	0.176	3.313
WHBC	4.299	0.005	21.686

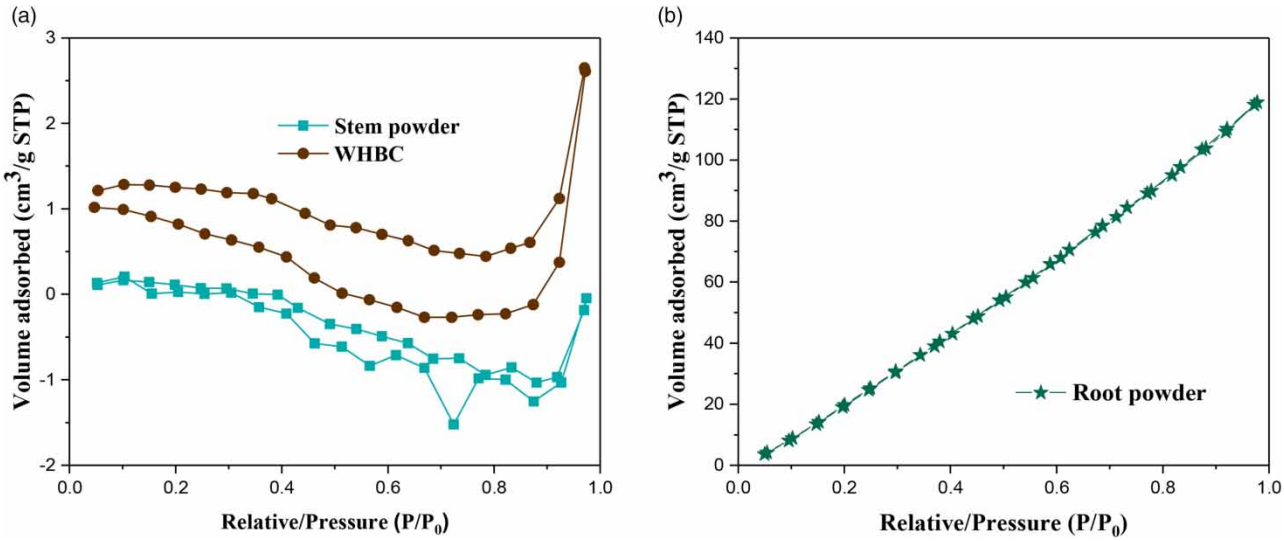

Figure 7 | N_2 adsorption-desorption curves of (a) the stem powder and the water hyacinth biochar (WHBC), and (b) the root powder.

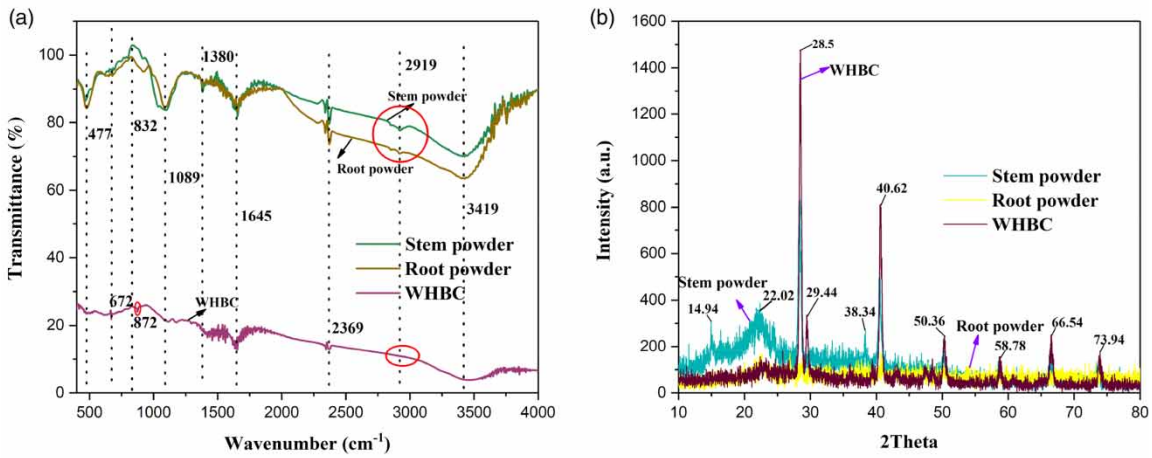

Figure 8 | Fourier-transform infrared spectroscopy (FTIR) spectra and X-ray diffraction (XRD) patterns of the three adsorbents: (a) FTIR spectra, (b) XRD patterns.

However, the stretching vibration peaks of the stem powder and root powder were near 2,800 cm^{-1} and 2,900 cm^{-1}, respectively, and were absent for the WHBC. These two peaks were aliphatic C-H antisymmetric stretching vibrations that weakened or even disappeared in WHBC, indicating that the pyrolysis and dehydration of aliphatic groups occurred after high-temperature pyrolysis. Additionally, the transmittances of the stem powder and the root powder near 2,369 cm^{-1}, 1,645 cm^{-1}, 1,089 cm^{-1}, and 832 cm^{-1} were higher than those of the WHBC, and their intensity in the WHBC decreased. For WHBC, the bands corresponding to the C-O stretching frequencies (1,645 cm^{-1}) of carboxyl, aldehyde, ketone, or ester groups, C-H bending (1,380 cm^{-1}) in alkanes and alkyl groups, C-H bending in alkenes (832 cm^{-1}), and out-of-plane N-H bending vibrations (672 cm^{-1}) gradually weakened or disappeared, suggesting that aliphatic compounds were highly aromatized during the carbonization process (Jin *et al.* 2021b). A new peak at 872 cm^{-1} appeared in the WHBC. This peak may be associated with the stretching and bending motions of CO_3^{2-}, which generates precipitates with heavy metal cations. This may also have been a reason why the adsorption performance of WHBC was stronger than those of the stem powder and root powder.

XRD patterns of the three water hyacinth materials

X-ray diffraction (XRD) was used to identify possible crystalline precipitates formed on the surface of the material. The XRD patterns of the stem powder, root powder, and WHBC are shown in Figure 8(b). As can be seen from Figure 8(b), the stem powder was dominantly amorphous with two broad peaks at 2θ values around 14.94° and 22.02°. This was likely due to the crystallinity possessed by cellulose. These two broad peaks disappeared in the WHBC, indicating that cellulose in water hyacinth decomposed under pyrolysis. Compared with the stem and root powder, the intensity of the WHBC at 2θ=28.50° and 40.62° was enhanced. This indicated that the crystallization degree of WHBC was significantly enhanced, which was consistent with Deng *et al.* (2019). In addition, the results showed that the pyrolytic reaction improved the graphite crystal structure and graphitization degree of the biomass. As shown in Figure 8(b), WHBC had a peak at 2θ=29.44°, while there was no such peak in stem powder or root powder. Combined with EDS analysis, these findings suggest that the peak here may represent the presence of Ca compounds, such as CaC_2O_4 or $CaCO_3$, which can precipitate with heavy metal ions. According to the XRD and EDS analyses, the WHBC was further confirmed to contain K, Ca, and Mg. These elements can react with heavy metal ions.

CONCLUSION

In this study, a novel soil column washing system was established to simulate the environment of CTs, and an orthophosphate solution was used to wash the thermally modified CTs. The passivation effect of orthophosphate on heavy metals in CTs reduces the bioavailability of heavy metals in CTs and alleviates pollution due to CTs that occurs during the landfill process. In addition, the adsorption and interception of orthophosphate by thermally modified CTs reduces the concentration of orthophosphates in the tail water, which helps alleviate the water eutrophication caused by phosphate. The tail water was collected, and three water hyacinth materials were introduced to remove the heavy metal ions in the tail water. The 20 g/L WHBC solution showed effective removal for heavy metals. After advanced treatment by WHBC, the concentration removal rates ($R\%$) of Cu^{2+}, Cd^{2+}, and Zn^{2+} were 99.48, 94.94, and 94.84%, respectively, and the concentrations of the three heavy metal ions in the effluent were 0.68, 0.41, and 1.11 mg/L, respectively, which greatly reduced their potential threat to the environment. This scheme took advantage of the passivation of heavy metals by phosphorous substances combined with the affinity effect of heavy metals and phosphorous substances. It also took advantage of the synergistic purification effect of both to remove heavy metals and phosphates at the same time. Then, WHBC was used to remove heavy metals in the tail water to reduce subsequent heavy metal pollution to the greatest extent. This scheme not only reduces the bioavailability of heavy metals in CTs but also reduces the risk of water eutrophication and improves soil fertility in CT reservoirs.

Of course, this study has some limitations. For example, when washing the CTs, a speciation analysis of the heavy metal ions was not conducted. In future research, the forms of heavy metal ions will be analyzed and determined to obtain more theoretical support for tailing remediation projects. Future research could also focus on the extraction of heavy metals from saturated stem powder, root powder, and biochar for use as resources. This would avoid secondary pollution and provide a source of heavy metals as resources for secondary use. In addition, our research is still in the laboratory stage, and practical engineering applications are still a long way off.

ACKNOWLEDGEMENTS

This research was supported by the National Natural Science Foundation of China (51808001); the Natural Science Foundation of Anhui Province, China (1708085QB45, 1808085QE146, 2008085ME159); and the Anhui Polytechnic University Scientific Research Project (Xjky2020169); and Natural Science research project of Anhui Universities (No. KJ2021A0505). We thank LetPub (www.letpub.com) for its linguistic assistance during the preparation of this manuscript.

DATA AVAILABILITY STATEMENT

All relevant data are included in the paper or its Supplementary Information.

REFERENCES

Deng, J., Li, B., Xiao, Y., Ma, L., Wang, C. P., Lai-wang, B. & Shu, C. M. 2017 Combustion properties of coal gangue using thermogravimetry–Fourier transform infrared spectroscopy. *Applied Thermal Engineering* **116**, 244–252.

Deng, Y. Y., Huang, S., Laird, D. A., Wang, X. G. & Meng, Z. W. 2019 Adsorption behavior and mechanisms of cadmium and nickel on rice straw biochars in single- and binary-metal systems. *Chemosphere* **218**, 308–318.

Dong, L. J., Deng, S. J. & Wang, F. Y. 2020 Some developments and new insights for environmental sustainability and disaster control of tailings dam. *Journal of Cleaner Production* **269**, 122270.

Esmaeili, J., Aslani, H. & Onuaguluchi, O. 2020 Reuse potentials of copper mine tailings in mortar and concrete composites. *Journal of Materials in Civil Engineering* **32** (5), 04020084.

Feizi, M. & Jalali, M. 2021 Leaching of Cd, Cu, Ni and Zn in a sewage sludge-amended soil in presence of geo- and nano-materials. *Journal of Cleaner Production* **297**, 126506.

Feng, W. J., Zhang, S. R., Zhong, Q. M., Wang, G. Y., Pan, X. M., Xu, X. X., Zhou, W., Li, T., Luo, L. & Zhang, Y. Z. 2020 Soil washing remediation of heavy metal from contaminated soil with EDTMP and PAA: properties, optimization, and risk assessment. *Journal of Hazardous Materials* **381**, 120997.

Gao, R. L., Hu, H. Q., Fu, Q. L., Li, Z. H., Xing, Z. Q., Ali, U., Zhu, J. & Liu, Y. H. 2020 Remediation of Pb, Cd, and Cu contaminated soil by co-pyrolysis biochar derived from rape straw and orthophosphate: speciation transformation, risk evaluation and mechanism inquiry. *Science of the Total Environment* **730**, 139119.

Jin, H. Y., Lin, L., Meng, X. Y., Wang, L. L., Huang, Z., Liu, M., Dong, L., Hu, Y. & Crittenden, J. C. 2021a A novel lanthanum-modified copper tailings adsorbent for phosphate removal from water. *Chemosphere* **281**, 130779.

Jin, Y., Zhang, M., Jin, Z. H., Wang, G. L., Li, R., Zhang, X., Liu, X. S., Qu, J. J. & Wang, H. M. 2021b Characterization of biochars derived from various spent mushroom substrates and evaluation of their adsorption performance of Cu(II) ions from aqueous solution. *Environmental Research* **196**, 110323.

Kaur, P., Kaur, P. & Kaur, K. 2020 Adsorptive removal of imazethapyr and imazamox from aqueous solution using modified rice husk. *Journal of Cleaner Production* **244**, 118699.

Lam, E. J., Zetola, V., Ramírez, Y., Montofre, I. L. & Pereira, F. 2020 Making paving stones from copper mine tailings as aggregates. *International Journal of Environmental Research and Public Health* **17**, 2448.

Melliti, A., Srivastava, V., Kheriji, J., Sillanpää, M. & Hamrouni, B. 2021 Date Palm Fiber as a novel precursor for porous activated carbon: optimization, characterization and its application as Tylosin antibiotic scavenger from aqueous solution. *Surfaces and Interfaces* **24**, 101047.

Munir, M. A. M., Liu, G. J., Yousaf, B., Mian, M. M., Ali, M. U., Ahmed, R., Cheema, A. I. & Naushade, M. 2020 Contrasting effects of biochar and hydrothermally treated coal gangue on leachability, bioavailability, speciation and accumulation of heavy metals by rapeseed in copper mine tailings. *Ecotoxicology and Environmental Safety* **191**, 110244.

Rahman, A., Hango, H. J., Daniel, L. S., Veikko, U., Jaime, S. J., Bhaskaruni, S. V. H. S. & Jonnalagadda, S. B. 2019 Chemical preparation of activated carbon from *Acacia erioloba* seed pods using H_2SO_4 as impregnating agent for water treatment: an environmentally benevolent approach. *Journal of Cleaner Production* **237**, 117689.

Raklami, A., Tahiri, A., Bechtaoui, N., Abdelhay, E. G., Pajuelo, E., Baslam, M., Meddich, A. & Oufdou, K. 2021 Restoring the plant productivity of heavy metal-contaminated soil using phosphate sludge, marble waste, and beneficial microorganisms. *Journal of Environmental Science* **99**, 210–221.

Song, L. Z., Huo, J. B., Wang, X. L., Yang, F. F., He, J. & Li, C. Y. 2016 Phosphate adsorption by a Cu(II)-loaded polyethersulfone-type metal affinity membrane with the presence of coexistent ions. *Chemical Engineering Journal* **284**, 182–193.

Tchatchouang, C. D., Ngueutchoua, G., Henock, D. E., Zacharie, A. E. B., Flodore, G. Y. G., Joël, U. F. B., Fouateu, R. Y., Carole, S. N. & Armstrong-Altrin, J. S. 2021 Distributions of trace metals and radionuclides contamination in alluvial sediments from the Lobé River in Cameroon. *Earth Systems and Environment*. https://doi.org/10.1007/s41748-021-00251-4.

Teng, Z. D., Zhao, X., Yuan, J. J., Li, M. & Li, T. G. 2021 Phosphate functionalized iron based nanomaterials coupled with phosphate solubilizing bacteria as an efficient remediation system to enhance lead passivation in soil. *Journal of Hazardous Materials* **419**, 126433. https://doi.org/10.1016/j.jhazmat.2021.126433.

Wang, P., Sun, Z. H., Hu, Y. A. & Cheng, H. F. 2019 Leaching of heavy metals from abandoned mine tailings brought by precipitation and the associated environmental impact. *Science of the Total Environment* **695**, 133893.

Wang, D. H., Li, G. H., Qin, S. Q., Tao, W. W., Gong, S. H. & Wang, J. 2021 Remediation of Cr(VI)-contaminated soil using combined chemical leaching and reduction techniques based on hexavalent chromium speciation. *Ecotoxicology and Environmental Safety* **208**, 111734.

Yin, S. H., Shao, Y. J., Wu, A. X., Wang, H. J., Liu, X. H. & Wang, Y. 2020 A systematic review of paste technology in metal mines for cleaner production in China. *Journal of Cleaner Production* **247**, 119590.

Zeng, Q., Wang, S. X., Hu, L., Zhong, H., He, Z. G., Sun, W. & Xiong, D. L. 2021 Oxalic acid modified copper tailings as an efficient adsorbent with super high capacities for the removal of Pb^{2+}. *Chemosphere* **263**, 127833.

Zhou, R. J., Wang, Y. B., Zhang, M., Li, J., Gui, Y. N., Tang, Y. Y., Yu, P. X. & Yang, Y. R. 2018 Effect of heating temperature and time on phosphate adsorption capacity of thermally modified copper tailings. *Water Science Technology* **77** (11), 2668–2676.

Zhou, R. J., Wang, Y. B., Zhang, M., Yu, P. X. & Li, J. Y. 2019 Adsorptive removal of phosphate from aqueous solutions by thermally modified copper tailings. *Environmental Monitoring and Assessment* **191** (4), 198–210.

Zhou, R. J., Zhang, M., Li, J. Y. & Zhao, W. 2020 Optimization of preparation conditions for biochar derived from water hyacinth by using response surface methodology (RSM) and its application in Pb^{2+} removal. *Journal of Environmental Chemical Engineering* **8** (5), 104198. https://doi.org/10.1016/j.jece.2020.104198.

First received 21 July 2021; accepted in revised form 17 January 2022. Available online 29 January 2022